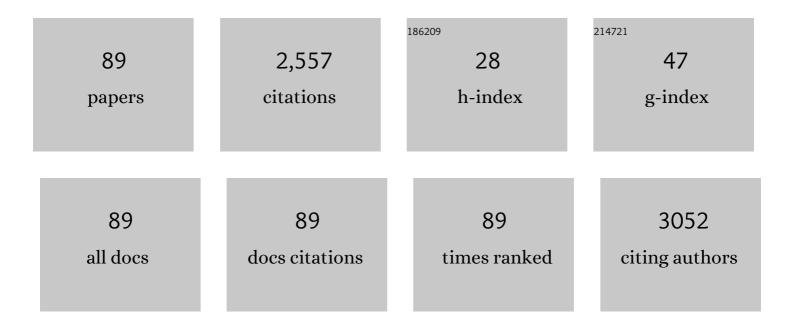


List of Publications by Year in descending order

Source: https://exaly.com/author-pdf/9546818/publications.pdf Version: 2024-02-01



VINCLI

#	Article	IF	CITATIONS
1	Direct Synthesis of Alâ^'SBA-15 Mesoporous Materials via Hydrolysis-Controlled Approach. Journal of Physical Chemistry B, 2004, 108, 9739-9744.	1.2	236
2	Direct synthesis of highly ordered Fe-SBA-15 mesoporous materials under weak acidic conditions. Microporous and Mesoporous Materials, 2005, 84, 41-49.	2.2	181
3	Hydrothermally Stable Thioether-Bridged Mesoporous Materials with Void Defects in the Pore Walls. Advanced Functional Materials, 2005, 15, 1297-1302.	7.8	107
4	Treatment of the potent greenhouse gas, CHF3—An overview. Journal of Fluorine Chemistry, 2012, 140, 7-16.	0.9	79
5	Enhanced Hydrogenation Performance over Hollow Structured Co oO <i>x</i> @N Capsules. Advanced Science, 2019, 6, 1900807.	5.6	79
6	Defect-rich activated carbons as active and stable metal-free catalyst for acetylene hydrochlorination. Carbon, 2019, 146, 406-412.	5.4	78
7	Dual-functional click-triazole: a metal chelator and immobilization linker for the construction of a heterogeneous palladium catalyst and its application for the aerobic oxidation of alcohols. Chemical Communications, 2012, 48, 2979.	2.2	77
8	Effect of Aluminum on the Nature of the Iron Species in Fe-SBA-15. Journal of Physical Chemistry B, 2006, 110, 26114-26121.	1.2	69
9	Pore size design of ordered mesoporous silicas by controlling micellar properties of triblock copolymer EO20PO70EO20. Microporous and Mesoporous Materials, 2006, 89, 179-185.	2.2	69
10	Enzyme confined in silica-based nanocages for biocatalysis in a Pickering emulsion. Chemical Communications, 2013, 49, 9558.	2.2	66
11	Synthesis of bifunctionalized mesoporous organosilica spheres for high-performance liquid chromatography. Journal of Chromatography A, 2006, 1103, 257-264.	1.8	65
12	Hydrothermal Stability and Catalytic Activity of Aluminum-Containing Mesoporous Ethaneâ^'Silicas. Journal of Physical Chemistry B, 2004, 108, 7934-7937.	1.2	57
13	Highly ordered periodic mesoporous ethanesilica synthesized under neutral conditions. Journal of Materials Chemistry, 2005, 15, 2562.	6.7	53
14	Wheat flour-derived N-doped mesoporous carbon extrudate as superior metal-free catalysts for acetylene hydrochlorination. Chemical Communications, 2018, 54, 623-626.	2.2	50
15	Effect of acidity and ruthenium species on catalytic performance of ruthenium catalysts for acetylene hydrochlorination. Catalysis Science and Technology, 2018, 8, 6143-6149.	2.1	48
16	Surface functionalization of SBA-15-ordered mesoporous silicas: Oxidation of benzene to phenol by nitrous oxide. Journal of Catalysis, 2008, 255, 190-196.	3.1	46
17	An efficient route for the preparation of activated carbon supported ruthenium catalysts with high performance for ammonia synthesis. Catalysis Today, 2011, 174, 97-105.	2.2	44
18	N-doped carbon spheres impregnated with highly monodispersed ruthenium nanoparticles as a hydrogenation catalyst. Chemical Engineering Journal, 2019, 374, 895-903.	6.6	44

#	Article	IF	CITATIONS
19	Solid state synthesis of Ru–MC with highly dispersed semi-embedded ruthenium nanoparticles in a porous carbon framework for benzoic acid hydrogenation. Catalysis Science and Technology, 2016, 6, 7259-7266.	2.1	41
20	Defective graphene@diamond hybrid nanocarbon material as an effective and stable metal-free catalyst for acetylene hydrochlorination. Chemical Communications, 2019, 55, 1430-1433.	2.2	41
21	Direct synthesis of nitrogen-doped mesoporous carbons for acetylene hydrochlorination. Chinese Journal of Catalysis, 2016, 37, 1242-1248.	6.9	40
22	Role of surface defects of carbon nanotubes on catalytic performance of barium promoted ruthenium catalyst for ammonia synthesis. Journal of Energy Chemistry, 2020, 41, 79-86.	7.1	39
23	Controlled synthesis of highly dispersed semi-embedded ruthenium nanoparticles in porous carbon framework with more exposed active sites. Catalysis Communications, 2012, 20, 29-35.	1.6	38
24	Direct synthesis of mesoporous nitrogen doped Ru-carbon catalysts with semi-embedded Ru nanoparticles for acetylene hydrochlorination. Microporous and Mesoporous Materials, 2018, 264, 248-253.	2.2	38
25	Synthesis and Characterization of Phosphonic Acid Functionalized Organosilicas with Bimodal Nanostructure. Chemistry of Materials, 2005, 17, 3019-3024.	3.2	35
26	Direct Synthesis of Ruthenium ontaining Ordered Mesoporous Carbon with Tunable Embedding Degrees by Using a Boric Acidâ€Assisted Approach. ChemCatChem, 2014, 6, 353-360.	1.8	31
27	Synthesis of mesoporous aluminosilicates with low Si/Al ratios using a single-source molecular precursor under acidic conditions. Journal of Porous Materials, 2006, 13, 187-193.	1.3	29
28	Iron-functionalized Al-SBA-15 for benzene hydroxylation. Chemical Communications, 2008, , 774-776.	2.2	29
29	Controlling Reaction Pathways for Alcohol Dehydration and Dehydrogenation over FeSBA-15 Catalysts. Catalysis Letters, 2007, 117, 18-24.	1.4	28
30	Quasi metal organic framework with highly concentrated Cr2O3 molecular clusters as the efficient catalyst for dehydrofluorination of 1,1,1,3,3-pentafluoropropane. Applied Catalysis B: Environmental, 2019, 257, 117939.	10.8	28
31	Enhancement of α-oxygen formation and N2O decomposition on Fe/ZSM-5 catalysts by extraframework Al. Chemical Communications, 2004, , 2480-2481.	2.2	27
32	Preparation and characterization of ordered mesoporous carbons on SBA-15 template. Journal of Materials Chemistry, 2006, 16, 1350.	6.7	27
33	Activation of a Carbon Support Through a Twoâ€Step Wet Oxidation and Highly Active Ruthenium–Activated Carbon Catalysts for the Hydrogenation of Benzene. ChemCatChem, 2014, 6, 572-579.	1.8	24
34	The origin of the extraordinary stability of mercury catalysts on the carbon support: the synergy effects between oxygen groups and defects revealed from a combined experimental and DFT study. Chinese Journal of Catalysis, 2019, 40, 141-146.	6.9	23
35	Solution combustion synthesis of nano-chromia as catalyst for the dehydrofluorination of 1,1-difluoroethane. Journal of Materials Science, 2016, 51, 11002-11013.	1.7	22
36	Microwave assisted combustion of phytic acid for the preparation of Ni ₂ P@C as a robust catalyst for hydrodechlorination. Chemical Communications, 2019, 55, 9279-9282.	2.2	22

#	Article	IF	CITATIONS
37	A highly stable and active mesoporous ruthenium catalyst for ammonia synthesis prepared by a RuCl3/SiO2-templated approach. Chinese Journal of Catalysis, 2019, 40, 114-123.	6.9	22
38	Effect of the graphitic degree of carbon supports on the catalytic performance of ammonia synthesis over Ba-Ru-K/HSGC catalyst. Journal of Energy Chemistry, 2014, 23, 443-452.	7.1	21
39	Promotion of Nb2O5 on the wustite-based iron catalyst for ammonia synthesis. Applied Surface Science, 2015, 353, 17-23.	3.1	21
40	Screening of active center and reactivity descriptor in acetylene hydrochlorination on metal-free doped carbon catalysts from first principle calculations. Applied Surface Science, 2019, 478, 574-580.	3.1	21
41	Reverting fluoroform back to chlorodifluoromethane and dichlorofluoromethane: Intermolecular Cl/F exchange with chloroform at moderate temperatures. Chemical Engineering Journal, 2019, 355, 594-601.	6.6	19
42	Generalized reactivity descriptor of defective carbon catalysts for acetylene hydrochlorination: the ratio of sp ² : sp ³ hybridization. Chemical Communications, 2020, 56, 14877-2	14880.	19
43	Direct Hydrothermal Synthesis of Iron-Containing Mesoporous Silica SBA-15: Potential as a Support for Gold Nanoparticles. Journal of Physical Chemistry C, 2009, 113, 21831-21839.	1.5	18
44	Solution Combustion Synthesis of Cr2O3 Nanoparticles and the Catalytic Performance for Dehydrofluorination of 1,1,1,3,3-Pentafluoropropane to 1,3,3,3-Tetrafluoropropene. Molecules, 2019, 24, 361.	1.7	18
45	Aluminium-containing mesoporous benzene-silicas with crystal-like pore wall structure. Journal of Materials Chemistry, 2005, 15, 4268.	6.7	17
46	Mesoporous aluminosilicates synthesized with single molecular precursor (sec-BuO)2AlOSi(OEt)3 as aluminum source. Microporous and Mesoporous Materials, 2006, 91, 85-91.	2.2	17
47	Simple synthesis of semi-graphitized ordered mesoporous carbons with tunable pore sizes. New Carbon Materials, 2011, 26, 123-129.	2.9	17
48	Geometric effect of Ru/HSAG@mSiO ₂ : a catalyst for selective hydrogenation of cinnamaldehyde. RSC Advances, 2014, 4, 30180-30185.	1.7	17
49	Improved catalytic performance of encapsulated Ru nanowires for aqueous-phase Fischer–Tropsch synthesis. Catalysis Science and Technology, 2016, 6, 2181-2187.	2.1	17
50	Catalytic pyrolysis of CHF3 over activated carbon and activated carbon supported potassium catalyst. Journal of Fluorine Chemistry, 2010, 131, 698-703.	0.9	16
51	SiO2-template synthesis of mesoporous MgF2 highly effective for Cl/F exchange reaction. Journal of Fluorine Chemistry, 2013, 150, 46-52.	0.9	16
52	Preparation of N-doped ordered mesoporous carbon and catalytic performance for the pyrolysis of 1-chloro-1,1-difluoroethane to vinylidene fluoride. Microporous and Mesoporous Materials, 2019, 275, 200-206.	2.2	16
53	Highly stable Ru nanoparticles incorporated in mesoporous carbon catalysts for production of \hat{I}^3 -valerolactone. Catalysis Today, 2020, 351, 75-82.	2.2	16
54	Effects of Reaction Conditions on Performance of Ru Catalyst and Iron Catalyst for Ammonia Synthesis. Chinese Journal of Chemical Engineering, 2011, 19, 273-277.	1.7	15

#	Article	IF	CITATIONS
55	Wheat flour-derived N-doped mesoporous carbon extrudes as an efficient support for Au catalyst in acetylene hydrochlorination. Chinese Journal of Catalysis, 2018, 39, 1664-1671.	6.9	15
56	Single-Site Au/Carbon Catalysts with Single-Atom and Au Nanoparticles for Acetylene Hydrochlorination. ACS Applied Nano Materials, 2020, 3, 3004-3010.	2.4	15
57	Confinement of AIF3 in MOF derived structures for the formation of 4-fold coordinated Al and significantly improved dehydrofluorination activity. Chemical Engineering Journal, 2020, 394, 124946.	6.6	15
58	Effect of pore structure of mesoporous carbon on its supported Ru catalysts for ammonia synthesis. Chinese Journal of Catalysis, 2013, 34, 1395-1401.	6.9	13
59	Preparation of fluorinated Cr2O3 hexagonal prism and catalytic performance for the dehydrofluorination of 1,1-difluoroethane to vinyl fluoride. Journal of Nanoparticle Research, 2015, 17, 1.	0.8	13
60	Î ³ -Fe2O3 as the precursor of iron based catalyst prepared by solid-state reaction at room temperature for Fischer-Tropsch to olefins. Applied Catalysis A: General, 2019, 572, 158-167.	2.2	13
61	Catalytic activity of Ru supported on SmCeOx for ammonia decomposition: The effect of Sm doping. Journal of Solid State Chemistry, 2021, 295, 121946.	1.4	13
62	Dibenzodioxin Adsorption on Inorganic Materials. Langmuir, 2005, 21, 3877-3880.	1.6	11
63	Strong Interaction of Ruthenium Species with Graphite Structure for the Self-Dispersion of Ru under Solvent-Free Conditions. ACS Sustainable Chemistry and Engineering, 2017, 5, 7195-7202.	3.2	10
64	Effect of nitrogen co-doping with ruthenium on the catalytic performance of Ba/Ru–N-MC catalysts for ammonia synthesis. RSC Advances, 2019, 9, 22045-22052.	1.7	10
65	Experimental and DFT Mechanistic Study of Dehydrohalogenation of 1-Chloro-1,1-difluoroethane over Metal Fluorides. Industrial & Engineering Chemistry Research, 2019, 58, 18149-18159.	1.8	10
66	Synergistic catalysis of carbon-partitioned LaF ₃ –BaF ₂ composites for the coupling of CH ₄ with CHF ₃ to VDF. Catalysis Science and Technology, 2019, 9, 1338-1348.	2.1	10
67	Yolk–shell nanospheres with soluble amino-polystyrene as a reservoir for Pd NPs. RSC Advances, 2015, 5, 35730-35736.	1.7	8
68	PVDF mediated fabrication of freestanding AlF3 sub-microspheres: Facile and controllable synthesis of α, β and θ-AlF3. Materials Chemistry and Physics, 2020, 240, 122287.	2.0	8
69	Homogeneously dispersed gold nanoparticles stabilized on the walls of ordered mesoporous carbon via a simple and repeatable method with enhanced hydrogenation properties for nitro-group. Microporous and Mesoporous Materials, 2013, 173, 189-196.	2.2	7
70	Easy synthesis of iron doped ordered mesoporous carbon with tunable pore sizes. Journal of Natural Gas Chemistry, 2012, 21, 275-281.	1.8	6
71	Formation mechanism of highly dispersed semi-embedded ruthenium nanoparticles in porous carbon matrix determined by in situ temperature-programmed infrared spectroscopy. Chinese Journal of Catalysis, 2018, 39, 146-156.	6.9	6
72	Rational design of MgF ₂ catalysts with long-term stability for the dehydrofluorination of 1,1-difluoroethane (HFC-152a). RSC Advances, 2019, 9, 23744-23751.	1.7	6

#	Article	IF	CITATIONS
73	Thermally conductive SiC as support of aluminum fluoride for the catalytic dehydrofluorination reaction. Catalysis Communications, 2020, 142, 106033.	1.6	6
74	Preparation of efficient ruthenium catalysts for ammonia synthesis via high surface area graphite dispersion. Reaction Kinetics, Mechanisms and Catalysis, 2014, 113, 361-374.	0.8	5
75	The reaction mechanism of acetylene hydrochlorination on defective carbon supported ruthenium catalysts identified by DFT calculations and experimental approaches. Inorganic Chemistry Frontiers, 2022, 9, 458-467.	3.0	5
76	Effect of Sulfuric Acid on Textural Properties and Catalytic Performance of Ruthenium-Containing Ordered Mesoporous Carbon Prepared via a Direct RuCl ₃ /SBA-15 Hard Templated Method. Journal of Nanoscience and Nanotechnology, 2014, 14, 7131-7138.	0.9	4
77	Facile Preparation of BaClxFy for the Catalytic Dehydrochlorination of 1-Chloro-1,1-Difluoroethane to Vinylidene Fluoride. Catalysts, 2020, 10, 377.	1.6	4
78	One-step Synthesis of N-Doped Mesoporous Carbon as Highly Efficient Support of Pd Catalyst for Hydrodechlorination of 2,4-Dichlorophenol. Chemical Research in Chinese Universities, 2018, 34, 1004-1008.	1.3	3
79	Catalytic Performance of Bi-functional WC/HZSM-5 Catalysts for <i>n</i> -Hexane Aromatization. Chinese Journal of Catalysis, 2013, 33, 570-575.	6.9	3
80	The in situ redispersion of a PdCu/AC alloy catalyst under a CFCl2CF2Cl/H2 atmosphere: a combination of experimental and DFT study. Chemical Communications, 2020, 56, 12001-12004.	2.2	2
81	Pyrolysis of Trifluoromethane over Activated Carbon: Role of the Surface Oxygen Groups. Progress in Reaction Kinetics and Mechanism, 2014, 39, 38-52.	1.1	1
82	Preparation and characterization of chromium-doped magnesium fluoride catalysts via an aqueous sol–gel method. Journal of Sol-Gel Science and Technology, 2019, 92, 200-207.	1.1	1
83	One-Pot Cascade Catalysis of Dehydrochlorination of Greenhouse Gas HCFC-142b and Hydrochlorination of Acetylene for the Spontaneous Production of VDF and VCM. ACS ES&T Engineering, 2022, 2, 121-128.	3.7	1
84	Experimental Study on Degradation of 1Cr5Mo Steel Tubes in the Coking Furnace at Super Temperature. Key Engineering Materials, 2007, 345-346, 1067-1070.	0.4	0
85	Diffusion LMS algorithm in wireless sensor networks with multiplicative input noise. , 2017, , .		0
86	Effect of Boron Nitride Support on Catalytic Activity of Ru-Ba/BN for Ammonia Synthesis. Chinese Journal of Catalysis, 2010, 31, 677-682.	6.9	0
87	Effect of Hydrothermal Treatment of Activated Carbon by Nitric Acid on Activ-ity of Ba-Ru-K/AC Catalyst for Ammonia Synthesis. Chinese Journal of Catalysis, 2013, 33, 1191-1197.	6.9	0
88	Effect of Cr-doping on the acidity and pore structure of mesoporous magnesium fluoride. Chinese Journal of Catalysis, 2014, 34, 373-378.	6.9	0
89	High-surface-area Magnesium Fluoride: Preparation by Template Method and Catalytic Activity for the Dehydrofluorination of HFC-152a. Wuji Cailiao Xuebao/Journal of Inorganic Materials, 2018, 33, 1186.	0.6	0